

## Article

# Characteristics of Hydro-Geochemistry and Groundwater Pollution in Songnen Plain in Northeastern China

Ruihui Chen <sup>1</sup>, Linmei Liu <sup>2</sup>, Yi Li <sup>3</sup>, Yuanzheng Zhai <sup>2</sup>, Haiyang Chen <sup>2</sup>, Bin Hu <sup>4</sup>, Qianru Zhang <sup>1</sup> and Yanguo Teng <sup>2,\*</sup>

- <sup>1</sup> Key Laboratory of Nonpoint Source Pollution Control, Ministry of Agriculture and Rural Affairs, Institute of Agricultural Resources and Regional Planning, Chinese Academy of Agricultural Sciences, Beijing 100081, China; chenruihui@caas.cn (R.C.); zhangqianru@caas.cn (Q.Z.)
- <sup>2</sup> College of Water Sciences, Beijing Normal University, Beijing 100875, China; 202021470017@mail.bnu.edu.cn (L.L.); zyz@bnu.edu.cn (Y.Z.); chen.haiyang@bnu.edu.cn (H.C.)
- <sup>3</sup> School of Civil Engineering, Architecture and Environment, Hubei University of Technology, Wuhan 430068, China; liyi\_bnuphd@mail.bnu.edu.cn
- <sup>4</sup> Research Center for Eco-Environmental Sciences, Chinese Academy of Sciences, Beijing 100045, China; binhu@rcees.ac.cn
- \* Correspondence: ygteng@bnu.edu.cn; Tel.: +86-010-58802796



**Citation:** Chen, R.; Liu, L.; Li, Y.; Zhai, Y.; Chen, H.; Hu, B.; Zhang, Q.; Teng, Y. Characteristics of Hydro-Geochemistry and Groundwater Pollution in Songnen Plain in Northeastern China. *Sustainability* **2022**, *14*, 6527. <https://doi.org/10.3390/su14116527>

Academic Editor: Fernando António Leal Pacheco

Received: 22 April 2022

Accepted: 24 May 2022

Published: 26 May 2022

**Publisher's Note:** MDPI stays neutral with regard to jurisdictional claims in published maps and institutional affiliations.



**Copyright:** © 2022 by the authors. Licensee MDPI, Basel, Switzerland. This article is an open access article distributed under the terms and conditions of the Creative Commons Attribution (CC BY) license (<https://creativecommons.org/licenses/by/4.0/>).

**Abstract:** Agricultural production may cause groundwater pollution. This study investigated the characteristics of shallow groundwater pollution in a typical black land agricultural production area in Northeastern China and the geochemical behavior of major pollutants. A total of 27 and 23 shallow groundwater samples were collected for measuring on-site parameters and major components in 2000 and 2014, respectively. The improved integrated approach was used to assess groundwater contamination. The results showed that the groundwater was slightly polluted by agricultural activities. The average concentrations of major ions of shallow groundwater were found to be in the following order:  $\text{Ca}^{2+} > \text{Na}^+ > \text{Mg}^{2+} > \text{K}^+$  for cations and  $\text{HCO}_3^- > \text{SO}_4^{2-} > \text{Cl}^- > \text{NO}_3^-$  for anions. Percentages of 7.4% and 34.8% of the total groundwater sample in 2000 and 2014, respectively, indicated that the shallow groundwater quality has gradually worsened in the past few decades. The concentration of  $\text{NO}_3^-$  was a major factor that influenced the observed groundwater quality changes. Scientific and effective fertilization of rice cultivation is an effective way to avoid groundwater pollution, and the improved groundwater quality evaluation methods can further improve the standard of groundwater resource management effectively.

**Keywords:** hydrogeochemical characteristics; groundwater pollution; quality assessment; groundwater management

## 1. Introduction

China's agricultural system is gradually shifting from traditional crude agriculture to modern efficiency-based agriculture [1,2]. Fertilizer application and tillage practices are the two main types of changes in agricultural production [3]. Modern agriculture is the embodiment of high yield, high quality, and high efficiency, and agricultural production is revitalized with the progress of productivity [4]. However, along with the rapid expansion of the agricultural cultivation area and the extension of the cultivation cycle, the highly intensive management of agricultural production has led to an imbalance in the supply and demand of water and heat, etc. in the agricultural cultivation area [4–6]. A series of groundwater and soil contamination problems have led to slow development in the agricultural production area in the Songnen Plain. This has become a major bottleneck limiting agricultural development. Northeast China is rich in black land resources and is an important food production area in the world [7]. High-intensity agricultural production has led to a continuous decline in soil fertility [7,8]. In order to ensure the sustainability

and stability of agricultural production, producers impose large amounts of agricultural fertilizers to maintain grain production. The Wuchang study area is a typical rice growing area in the Songnen Plain, and this study area is a typical northeastern black soil and is an important grain production base in northeast China. Excessive fertilizer use has led to the accumulation of chemical fertilizers in the soils of the Songnen Plain, and these excess fertilizer nutrients enter the groundwater system through rainwater infiltration, thus causing groundwater contamination [9].

Groundwater is the main source of daily domestic and agricultural water in the Songnen Plain [9,10]. As the main irrigation water, groundwater quality is related to agricultural production and environmental safety in the Tohoku region. In general, shallow groundwater is very susceptible to the influence of external production and construction practices [10,11]. The mineral components as well as dissolved nitrogen in shallow groundwater mainly come from the ground and human activities [12]. Previous studies on the environmental quality of groundwater in Northeast China are relatively limited [13–17]. Numerous studies have shown that the excess of dissolved ions and nitrogen in groundwater in the northeast is the main factor contributing to groundwater contamination in the northeast [15–19]. The aim of the present study is to investigate the possible sources of contamination and to conduct a study on the distribution characteristics of the main groundwater contaminants and the degree of groundwater contamination. Based on this, two groundwater pollution evaluation methods were improved and they were used to carry out a study of groundwater pollution in the Lalin River basin.

The security of drinking water is increasingly important for human activities [18–21]. Consequently, it is essential to assess groundwater quality in combination with an analysis of the hydrogeochemical characteristics in groundwater [22]. Methods such as the piper diagram and Gibbs plot have been used to show major ion chemistry in groundwater samples in many studies [23–25]. Groundwater quality in semi-humid and semi-arid regions is a vital factor affecting human health and the quantity and quality of farm products because it is directly associated with domestic and agricultural purposes. While the physicochemical quality of groundwater has been significantly influenced by anthropogenic activities, such as urban, industrial, and intensive agricultural development [25–32], high concentrations of  $\text{NO}_3^-$  in shallow groundwater have resulted from the excessive use of nitrogen fertilizer [33].

In previous studies, most researchers focused on the spatial variation in groundwater pollution and neglected the accuracy of the approved groundwater pollution evaluation [3–7,15–18,34]. In fact, the spatial distribution of groundwater pollution is dependent on the accuracy of pollution assessment and grading. The intercomparison between different methods can, on the one hand, improve the basis of the assessment and, on the other hand, ensure the accurate judgment of the groundwater pollution level at a certain point, which can help to further propose targeted remediation and protection proposals [35]. However, from the perspective of methodological sophistication, these quantitative analysis methods have been used for a long time, and the evaluation results may not be suitable for the needs of modern groundwater environmental management [34,35]. Although methods such as the water quality index, fuzzy evaluation method, and comprehensive evaluation method have been widely applied to evaluate groundwater quality [28–36], the levels of groundwater contamination calculated by the above methods are not accurate enough to meet the needs of scientific management. Therefore, these methods should be improved according to the characteristics of groundwater pollution evaluation and the needs of risk assessment, in order to adapt to the macro management needs of managers. Improved groundwater evaluation methods are more accurate and better suited for agricultural production.

Therefore, the main aim of this study is to investigate the characteristics of groundwater pollution in the study area and the applicability and effectiveness of improving comprehensive evaluation methods on the interpretation of groundwater quality and contamination assessment. The study area is located in Songnen Plain in northeastern

China, where groundwater is the major source for agricultural production. The objectives of this study are to: (1) recognize the hydrogeochemical characteristics and the main sources of groundwater chemical pollution; (2) compare the results and performance of each calculation method to provide reliable evaluation on groundwater contamination; (3) propose the main control and management recommendations according to the integrated calculation results.

## 2. Materials and Methods

### 2.1. Description of Study Area

The study area is located in the riverside source field of Lalin, the northeastern region of China, at a longitude between  $126^{\circ}58'$  and  $127^{\circ}07'$  E, and a latitude between  $45^{\circ}02'$  and  $45^{\circ}05'$  N, covering approximately  $100 \text{ km}^2$ . This area is located at the intersection of the Lalin River and Mangniu River (Figure 1). The study area is characterized by a temperate continental monsoon climate with a mean annual temperature of approximately  $3.6^{\circ}\text{C}$ . The summer maximum and winter minimum temperatures are  $36.5^{\circ}\text{C}$  and  $-40.9^{\circ}\text{C}$ , respectively. The mean annual precipitation is approximately  $619.7 \text{ mm}$ . The precipitation mainly occurs from June to August, accounting for 65–70% of the annual precipitation. The mean annual evaporation and the mean annual number of frost-free days are approximately  $1321.4 \text{ mm}$  and 179, respectively [6,7,13].

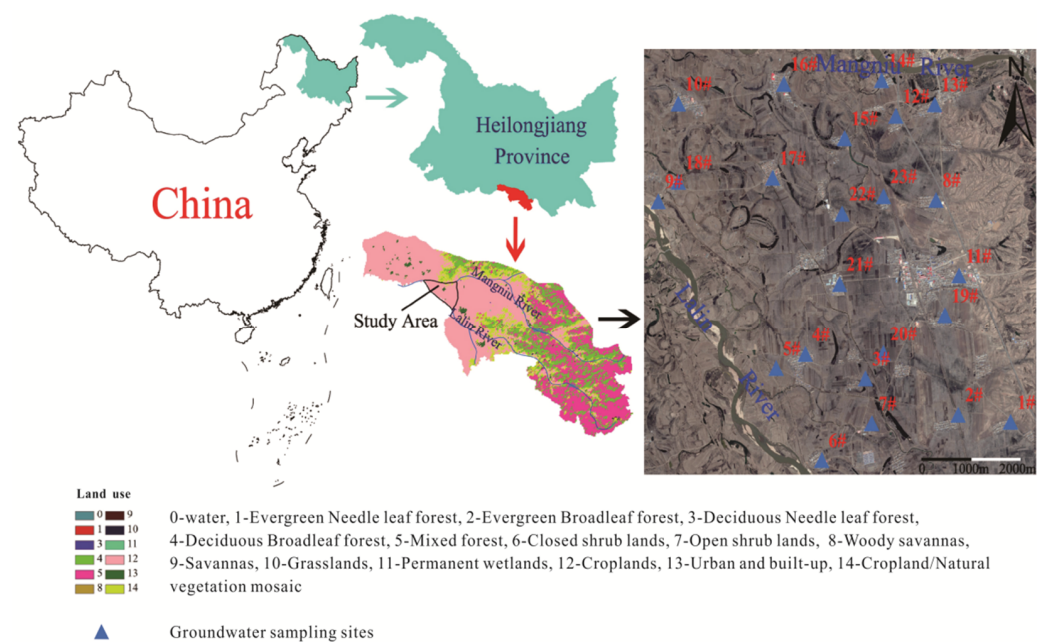


**Figure 1.** Study area and sampling sites of groundwater in the Lalin River Basin.

The primary aquifers in the Lalin River Basin are composed of Quaternary sediments with a thickness of 30–60 m, which is the main storage system of groundwater. Sandstone, pebbly medium-coarse sandstones, sand gravel, and gravel pebbles compose the main sediments. Based on the lithological properties, geological age, distribution of aquifers and aquitards, and hydrodynamic conditions, the Quaternary sediments are divided into the submersible water aquifer group and the confined water aquifer group. The submersible water aquifer thickens gradually from the south to north, with a thickness between 37.5 and 51 m. Vertically, the grain size changes from fine in the top to coarse in the bottom. Horizontally, the grain size changes slightly from east to west and varies from coarse to fine near the Lalin River. The thickness of the confined water aquifer is between 26.5 and 31 m. Vertically, it has the same regulation as the submersible water aquifer and has no apparent change in the horizontal direction. The aquifers are recharged by the infiltration

of precipitation, lateral flows, and agriculture irrigation infiltration and discharge mainly by artificial exploitation.

## 2.2. Sampling Collection and Analysis

The historical groundwater quality data used for this study were obtained from a report of the water source exploration in 2000, including twenty-seven groundwater samples taken in the dry season. An additional twenty-three shallow groundwater samples were collected in 2014 during the dry season. The parameters of electrical conductivity (EC), total dissolved solids (TDS), temperature, turbidity, pH, redox potential, conductivity, dissolved oxygen, and total dissolved solids were measured in the field using an Automatic Water Quality Monitor. Alkalinity was determined using acid–base titration. All of the inorganic water samples were filtered promptly after collection for an analysis of hydrochemical composition using 0.22  $\mu\text{m}$  membranes filters. Samples for major anion analysis were collected in 10 mL centrifuge tubes without acidification. Samples for cations and trace element analyses were preserved in 125 mL polyethylene bottles and were acidified to  $\text{pH} < 2$  with ultrapure  $\text{HNO}_3$  (1:1). Samples for volatile organic compounds (VOCs) were conserved in 40 mL brown glass bottles and acidified to  $\text{pH} < 2$  with HCl. Samples for semi-volatile organic compounds were stored in 1 L brown glass bottles. All of the organic water samples were stored at 4  $^\circ\text{C}$  until analysis.

## 2.3. Chemical Analyses

Concentrations of  $\text{Cl}^-$ ,  $\text{SO}_4^{2-}$ , and  $\text{NO}_3^-$  were determined by a High-Performance Ion Chromatograph (IC). Concentrations of  $\text{K}^+$ ,  $\text{Na}^+$ ,  $\text{Ca}^{2+}$ , and  $\text{Mg}^{2+}$  were measured by Inductively Coupled Plasma-Atomic Emission Spectrometry (ICP-AES). The analysis of volatile organic compounds and semi-volatile organic compounds was conducted using gas chromatography–mass spectrometry (GC–MS). The charge balance errors in all of the analyses were less than 10% [37].

## 2.4. Groundwater Quality Assessment Method

### 2.4.1. Comprehensive Evaluation Method

The comprehensive evaluation method has been widely used to assess groundwater quality for drinking purposes in China [7,8]. Four steps are followed to evaluate drinking water quality in the above method. In the first step, the indicators of groundwater, such as TH, TDS,  $\text{Cl}^-$ ,  $\text{SO}_4^{2-}$ , and  $\text{NO}_3^-$ , were selected to assess the groundwater quality in the study area. In the second step, according to the quality standard for the groundwater of China (GB/T 14848-93) (Table S1) [20], an evaluation score was assigned to each indicator of the groundwater samples by comparing its concentration to the classified indexes, as shown in Table S2. The comprehensive evaluation score ( $F$ ) was calculated by the following equations:

$$\bar{F} = \frac{1}{n} \sum_{i=1}^n F_i \quad (1)$$

$$F = \sqrt{\frac{\bar{F}^2 + F_{max}^2}{2}} \quad (2)$$

where  $F_i$  is the evaluation score of each parameter,  $i$  is the number of parameters,  $\bar{F}$  is the average evaluation score of  $F_i$ , and  $F_{max}$  is the maximum evaluation score of  $F_i$ . In the last step, the categories of the groundwater quality from Table S3 were determined by the value of  $F$ .

### 2.4.2. Improved Fuzzy Mathematical Method

First, it is necessary to establish the evaluation set, the identified  $m$  pollution components as evaluation factors, and the construction of the actual measurement and testing data set matrix  $C_i$  and evaluation criteria matrix  $S_{4 \times 5}$ . Secondly, it is necessary to determine the

evaluation index weights, the average value of the evaluation criteria as the cut-off point for dividing the pollution level, and the normalization of the fuzzy calculation. Finally, the affiliation degree and the improved affiliation degree need to be determined, and the affiliation degree vector can be obtained by compounding  $W$  with  $R$ . The improved type of the proposed affiliation degree calculates the comprehensive fuzzy evaluation index  $Z(k)$ , and the specific process is shown in the following equation:

$$C_i = [C_1, C_2, \dots, C_{n-1}, C_n] \quad (3)$$

$$S_{m \times n} = \begin{bmatrix} S_{11}, S_{12}, \dots, S_{1,n-1}, S_{1,n} \\ S_{21}, S_{22}, \dots, S_{2,n-1}, S_{2,n} \\ \dots \dots \dots \dots \\ S_{m1}, S_{m2}, \dots, S_{m,n-1}, S_{m,n} \end{bmatrix} \quad (4)$$

$$\begin{cases} S'_i = \frac{1}{u} \sum_{j=1}^n S_{ij} \\ C_i / S'_i \\ W_{1m} = Q_i / \sum_{i=1}^m Q_i \\ W_{1 \times m} = [w_{11}, w_{12}, \dots, w_{1,m}] \end{cases} \quad (5)$$

$$R_{ij} = \begin{bmatrix} 1, C_i \leq S_{ij} \\ \frac{C_i - S_{i(j+1)}}{S_{ij} - S_{i(j+1)}}, S_{ij} < C_i < S_{i(j+1)} \\ 0, C_i \geq S_{i(j+1)} \end{bmatrix} \quad j = 1 \quad (6)$$

$$R_{ij} = \begin{bmatrix} 1, C_i \leq S_{i(j+1)} \\ \frac{C_i - S_{i(j+1)}}{S_{ij} - S_{i(j+1)}}, S_{i(j+1)} < C_i < S_{ij} \\ \frac{C_i - S_{i(j+1)}}{S_{ij} - S_{i(j+1)}}, S_{ij} < C_i < S_{i(j+1)} \\ 0, C_i \geq S_{i(j+1)} \end{bmatrix} \quad 1 < j < n \quad (7)$$

$$R_{ij} = \begin{bmatrix} 0, C_i \leq S_{i(j-1)} \\ \frac{C_i - S_{i(j-1)}}{S_{ij} - S_{i(j-1)}}, S_{i(j-1)} < C_i \leq S_{ij} \\ 1, C_i > S_{ij} \end{bmatrix} \quad j = n \quad (8)$$

$$\begin{cases} Z(K) = \sum_{n=1}^1 n B_n^* / \sum_{n=1}^1 B_n^* \\ B_n^* = \frac{B_{n(x)} - \min B_{n(x)}}{\max B_{n(x)} - \min B_{n(x)}} \end{cases} \quad (9)$$

where  $C_i$  is the matrix of measured values of evaluation factors;  $S'_i$  is the average value of each criterion of the  $i$ th class of evaluation factors;  $u$  is the number of classes, which is set as  $n$ ;  $S_{ij}$  is the evaluation criterion value of the  $j$ th class corresponding to the  $i$ th class of evaluation factors;  $W_{1m}$  is the weight of the  $m$ th class of evaluation factors;  $k$  is the number of water samples;  $B_{n(x)}$  is the class affiliation of  $n$ .

#### 2.4.3. Gray Correlation Method

The entropy weight method was used to determine the index weights, and the original data matrix  $X$  composed of each evaluation index was normalized to obtain the judgment matrix  $Y$ . After that, the entropy value was defined, and the entropy weight was calculated according to the entropy value  $H_k$ . Finally, the weights obtained from the superscript assignment method and the entropy weight method were combined, and the weighted

correlation degree of the combined weights and gray functional areas determined by the superscript assignment method and the entropy weight method were calculated as follows:

$$y_{i(k)} = \frac{\max\{x_{i(k)}\} - x_{i(k)}}{\max\{x_{i(k)}\} - \min\{x_{i(k)}\}} \quad (10)$$

$$Y = \begin{bmatrix} y_{11} & y_{12} & \cdots & y_{1n} \\ \vdots & \vdots & & \vdots \\ y_{m1} & y_{m2} & \cdots & y_{mn} \end{bmatrix} \quad (11)$$

$$H_k = \frac{-\sum_{k=1}^n f_{i(k)} \ln f_{i(k)}}{\ln n} \quad (12)$$

$$f_{ik} = \left(1 + y_{i(k)}\right) / \sum_{k=1}^n \left(1 + y_{i(k)}\right) \quad (13)$$

$$w_{e(k)} = \frac{1 - H_k}{n - \sum_{k=1}^n H_k} \quad (14)$$

$$w_{i(k)} = \frac{w_{1(k)} - w_{e(k)}}{\sum_{k=1}^n w_{1(k)} w_{e(k)}} \quad (15)$$

$$r_i = \sum_{k=1}^n w_{i(k)} \zeta_{i(k)} \quad (16)$$

### 3. Results

#### 3.1. Hydrogeochemical Characteristics

##### 3.1.1. Geochemical Characteristics of Major Ions

All of the field measurement parameters and chemical compositions of shallow groundwater from 2014 were summarized by minimum, mean, and maximum values, as shown in Table S4. The temperatures in shallow groundwater varied from 7.1 to 12.2 °C, with a mean of 9.3 °C. The value of pH ranged from 6.5 to 8.1, with a mean of 7.4. The range of EC was between 151.2 and 865.0  $\mu\text{s}/\text{cm}$ , and correspondingly, the values of TDS ranged from 117.0 to 1319.7 mg/L, with a mean of 419.4 mg/L. The values of TDS in all of the samples except one were less than 1 g/L, indicating fresh water. TH, measured as  $\text{CaCO}_3$ , varied between 12.2 and 914.7 mg/L, with an average of 166.9 mg/L. All of the shallow groundwater samples were soft to hard water, except one sample.

Concentrations of organic components (VOCs, atrazine, parathion, dichlorvos, dimethoate, parathion-methyl, demeton, and malathion) were below the detection limits. However, all of the inorganic components in shallow groundwater were detected (Table S4). For the cations, the concentrations of  $\text{K}^+$ ,  $\text{Na}^+$ ,  $\text{Ca}^{2+}$ , and  $\text{Mg}^{2+}$  ranged between 0.9 and 27.1, 7.5 and 180.7, 12.3 and 149.7, and 2.2 and 44.9 mg/L, with means of 6.4, 36.2, 50.8, and 11.7 mg/L, respectively. Among the anions, the concentrations of  $\text{Cl}^-$ ,  $\text{SO}_4^{2-}$ ,  $\text{HCO}_3^-$ , and  $\text{NO}_3^-$  ranged from 3.9 to 292.5, 3.8 to 197.0, 22.2 to 309.0, and 0.1 to 323.1 mg/L, with means of 58.8, 66.2, 119.6, and 58.0 mg/L, respectively. In comparison with previous data from 2000, in the study area, the mean concentrations of  $\text{K}^+$ ,  $\text{Na}^+$ ,  $\text{Ca}^{2+}$ , and  $\text{Mg}^{2+}$  showed elevated values of 1.5, 11.7, 10.1, and 2.3 mg/L, respectively. The mean concentrations of  $\text{Cl}^-$ ,  $\text{SO}_4^{2-}$ ,  $\text{HCO}_3^-$ , and  $\text{NO}_3^-$  increased to 12.8, 28.9, 14.8, and 42.1 mg/L, respectively. Furthermore, Figure 2 showed that the concentrations of major ions in shallow groundwater obviously changed between 2000 and 2014.

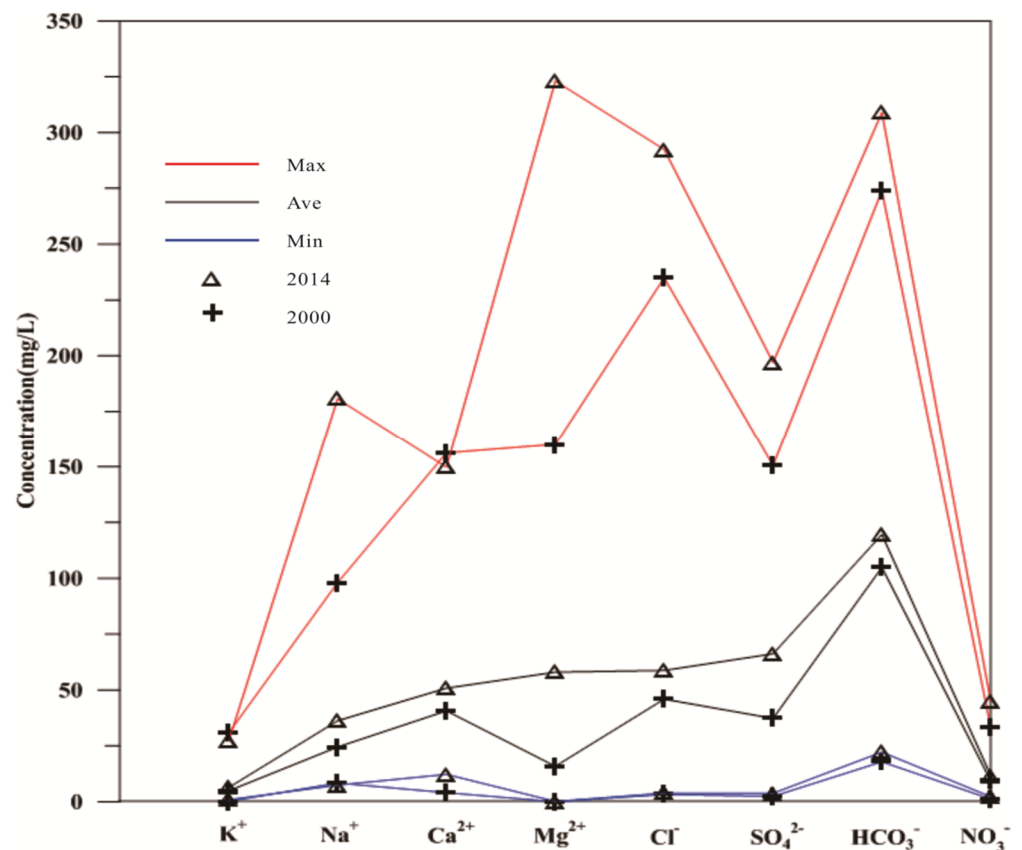


**Figure 2.** Distribution of the content for the main components of groundwater in the Lalin River Basin (Year 2014 and 2000).

### 3.1.2. Spatial Distribution of Major Ions

The spatial variation in the geochemical components in groundwater suggested that natural and anthropogenic activities were changed. The spatial distribution patterns of the major ions in the shallow groundwater of the studied area in 2014 were shown on the contour maps using the Kriging method (Figure 3).

The spatial distribution pattern of K<sup>+</sup> had no remarkable regularity, but a high concentration of K<sup>+</sup> occurred in wells 1#, 4#, 14#, and 23#. A higher concentration of Na<sup>+</sup> was found near the Lalin River (Figure 3). In contrast, the concentration of Na<sup>+</sup> was relatively low in the other studied zone. Similar distribution patterns were discovered for Ca<sup>2+</sup>, Mg<sup>2+</sup>, and HCO<sub>3</sub><sup>-</sup> (Figure 3), showing that the concentrations of ions increased from the Lalin River to the Mangniu River. The maximum concentrations of Ca<sup>2+</sup> and Mg<sup>2+</sup> were observed in well 4#, whereas the highest concentration of HCO<sub>3</sub><sup>-</sup> was observed around wells 1#, 8#, and 15#. The spatial pattern of Cl<sup>-</sup> was similar to that of Na<sup>+</sup>. The distribution pattern of SO<sub>4</sub><sup>2-</sup> showed a relatively high concentration close to the Lalin and Mangniu Rivers and gradually increased from the central zone to the two rivers. A relatively high concentration of NO<sub>3</sub><sup>-</sup> was observed in the study area, except around well 17#, and the maximum concentration of NO<sub>3</sub><sup>-</sup> was found in well 4#, followed by wells 10# and 11# (Figure 3). It could be seen that the concentrations of all of the major ions except HCO<sub>3</sub><sup>-</sup> were high in well 4#.

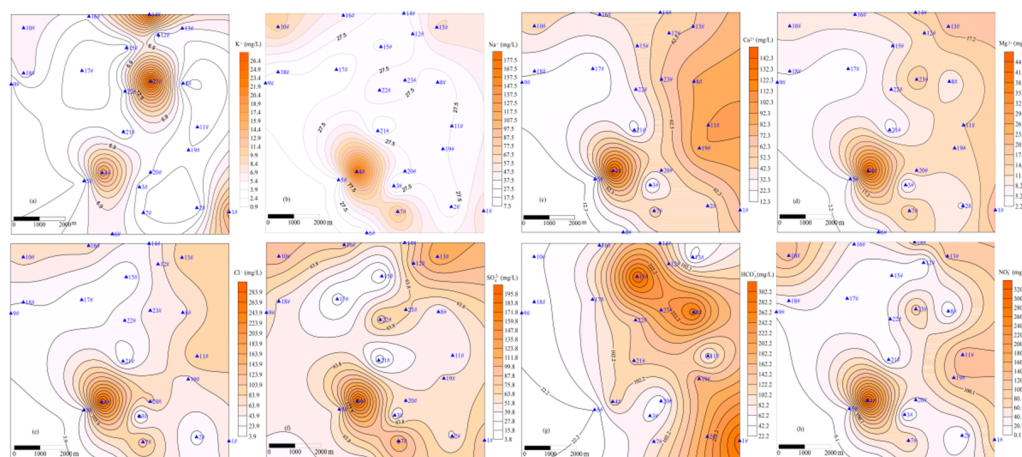


**Figure 3.** Spatial distribution for the main components of groundwater in the Lalin River Basin in 2014.

### 3.2. Source of Major Components

#### 3.2.1. Dissolution of Minerals Analysis

The Piper diagram was applied to illustrate studies of groundwater quality and geochemistry. The scatter distribution of the groundwater samples in the study area on the Piper diagram indicated that the hydrochemical facies in shallow groundwater changed slightly from 2000 to 2014 (Figure 4). With respect to cations, the samples of shallow groundwater from the two years were mainly spread over zones A and B of the lower left ternary region, except for one that was plotted in zone C, indicating that  $\text{Ca}^{2+}$ -type water was dominant, followed by mixed-type water. However, most of the samples for anions were distributed in zones E and B of the lower right ternary region, except for a few that were located in zones F and G, suggesting that  $\text{HCO}_3^-$ -type and mixed-type water were dominant, followed by  $\text{Cl}^-$ -type and  $\text{SO}_4^{2-}$ -type water. The distribution of the shallow groundwater samples in different subdivisions of the diamond-shaped region of the piper diagram uncovered the analogies and dissimilarities. The majority of the groundwater samples were situated in zones I and IV of the diamond-shaped region, except a few that were plotted in zone III, indicating that the hydrogeochemical facies of shallow groundwater were  $\text{Ca}^{2+} - \text{HCO}_3^-$  and mixed-type in 2000 and 2014 for the studied area, respectively. Meanwhile, samples distributed in zone I implied that the concentration of alkaline earth metals ( $\text{Ca}^{2+} + \text{Mg}^{2+}$ ) was greater than that of alkali metals ( $\text{Na}^+ + \text{K}^+$ ) in the study area and that the concentration of weak acid anions ( $\text{HCO}_3^- + \text{CO}_3^{2-}$ ) exceeded that of strong acid anions ( $\text{Cl}^- + \text{SO}_4^{2-}$ ) in the study area.

The saturation index (SI) was defined quantitatively as the deviation of water from equilibrium with respect to the mineral phases and was used to analyze the potential chemical reactions in the groundwater. The values of SI were zero, negative, and positive, implying that the water was exactly saturated, undersaturated, and oversaturated with the dissolved mineral, respectively. The values of SI for all of the samples in 2000 and 2014 were calculated using the geochemical model Aquachem 4.0. The SI values for calcite ( $\text{CaCO}_3$ ), dolomite ( $\text{CaMg}(\text{CO}_3)_2$ ), and aragonite ( $\text{CaCO}_3$ ) in shallow groundwater samples in 2014 varied from  $-1.90$  to  $0.46$ ,  $-4.18$  to  $0.46$ , and  $-2.06$  to  $0.31$ , with mean values of  $-0.78$ ,  $-2.08$ , and  $-0.94$ , respectively (Table 1). Approximately 87%, 96%, and 87% of the SI values of calcite, dolomite, and aragonite were less than zero, respectively. From the above SI values, the majority of samples were undersaturated with respect to calcite, dolomite, and aragonite. All of the values of SI for gypsum ( $\text{CaSO}_4$ ) and halite ( $\text{NaCl}$ ) were negative in the shallow groundwater, with average values of  $-2.07$  and  $-7.55$ , suggesting that all of the samples were undersaturated with respect to two minerals. Thus, the results implied that the dissolution of carbonate minerals could be the main source of monitored  $\text{Ca}^{2+}$ ,  $\text{Mg}^{2+}$ , and  $\text{HCO}_3^-$ ; the dissolution of halite may be responsible for the observed  $\text{Na}^+$



and  $\text{Cl}^-$ ; and the dissolution of gypsum was, to a certain extent, the source of  $\text{Ca}^{2+}$  and  $\text{SO}_4^{2-}$  to the shallow groundwater of the study area. From Table 1, sources of the major components in the shallow groundwater in 2000 were similar with those in 2014 according to calculations of the SI values.

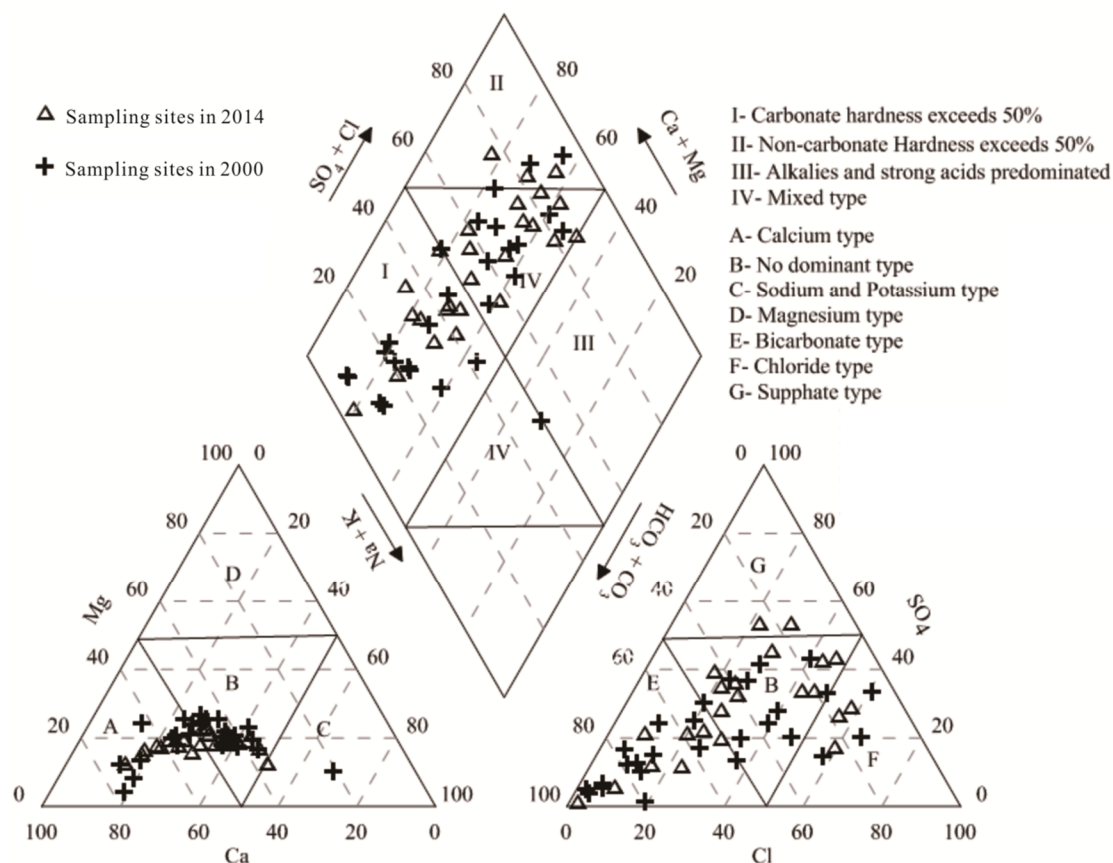


Figure 4. Piper diagram of groundwater in the Lalin River Basin in 2000 and 2014.

Table 1. Summary statistics of mineral SI of groundwater in the Lalin River Basin in 2000 and 2014.

No.	SI of Minerals	Minimum		Average		Maximum		Standard Deviation	
		2000	2014	2000	2014	2000	2014	2000	2014
1	Calcite	−2.65	−1.90	−0.95	−0.78	0.87	0.46	1.03	0.65
2	Dolomite	−5.58	−4.18	−2.26	−2.08	1.24	0.46	2.00	1.26
3	Gypsum	−3.38	−3.16	−2.46	−2.07	−1.41	−1.22	0.54	0.50
4	Halite	−9.09	−8.74	−7.93	−7.55	−6.31	−5.88	0.77	0.74
5	Aragonite	−2.80	−2.06	−1.10	−0.94	0.72	0.31	1.03	0.65

### 3.2.2. Water–Rock Interaction and Correlation Analysis

A Gibbs plot was used to analyze the functional source of the dissolved chemical components in the study area, differentiating the mechanisms of atmospheric-precipitation dominance, rock weathering dominance, and evaporation-crystallization dominance. The Gibbs log plot represented the ratios of  $\text{Na}^+ / (\text{Na}^+ + \text{Ca}^{2+})$  and  $\text{Cl}^- / (\text{Cl}^- + \text{HCO}_3^-)$  versus TDS, which have been widely applied to study hydro-geochemistry. Figure 5a,b clearly showed that samples in shallow groundwater in 2000 and 2014 were almost plotted on the shadow area, suggesting that the chemistry of the groundwater samples was dominantly influenced by rock weathering. In other words, evaporation-crystallization and atmospheric-precipitation played no apparent role in the shallow groundwater chemistry.

Furthermore, the variation in  $\text{Na}^+ / (\text{Na}^+ + \text{Ca}^{2+})$ , from low to high, was not accompanied with a large change in TDS (Figure 5), indicating that the rock weathering was also

affected by a cation-ion exchange interaction. The plot of  $\text{HCO}_3^-$  and  $\text{SO}_4^{2-}$ -corrected  $\text{Ca}^{2+}$  and  $\text{Mg}^{2+}$  versus  $\text{Cl}^-$ -corrected  $\text{Na}^+ + \text{K}^+$  was used to illustrate the extent of ion exchange, and the bivariate plot slope of  $-1$  with ion exchange between  $\text{Na}^+$  and  $\text{Ca}^{2+} + \text{Mg}^{2+}$  was determined by Jankowski et al [30]. The slope of the shallow groundwater samples in 2000 (Figure 6) was close to  $-1$ , indicating that ion exchange was a major source of shallow groundwater components. However, the slope of shallow groundwater samples in 2014 was  $-1.2$ , suggesting that concentrations of shallow groundwater components were not only influenced by ion exchange but also by the control of other actions. For example, the exchange of  $\text{Fe}^{2+}$  and  $\text{Mn}^{2+}$ , which are highly abundant in the strata of the region, led to an increase in slope.

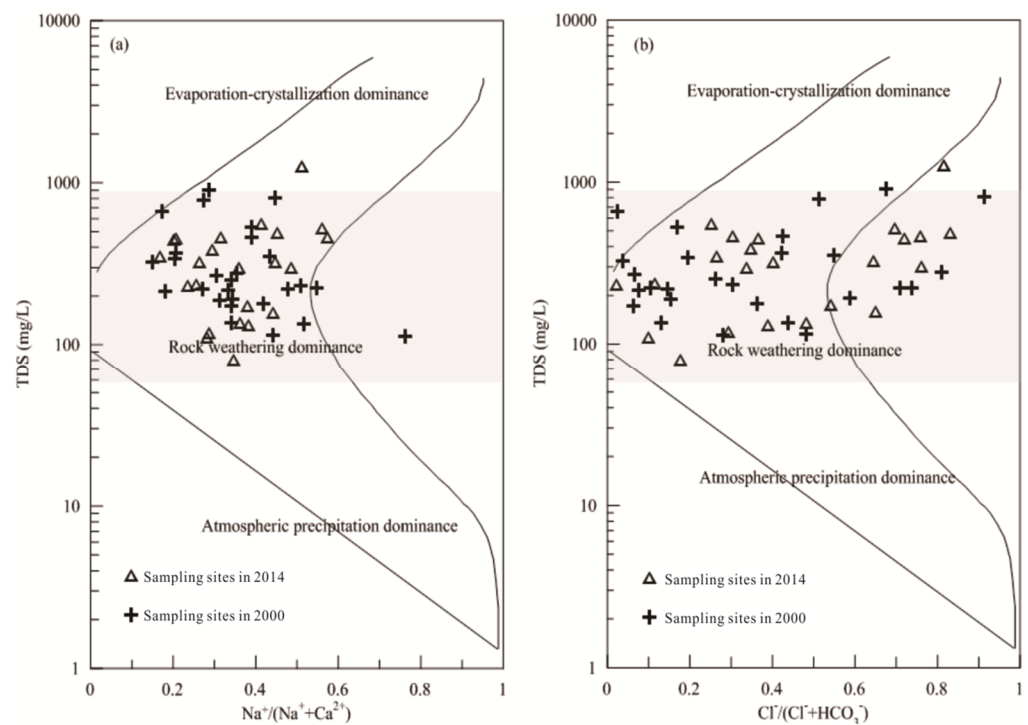


**Figure 5.** The Gibbs plot of TDS versus  $\text{Na}^+ / (\text{Na}^+ / \text{Ca}^{2+})$  (a) and TDS versus  $\text{Cl}^- / (\text{Cl}^- + \text{HCO}_3^-)$  (b) in the Lalin River Basin.

Figure S1 shows the correlation between environmental factors such as TDS, TH, T, and groundwater ions. From Figure S1, it can be found that the correlation between groundwater ions and environmental factors indexes was relatively small in 2000, which indicated that the groundwater in the area did not suffer from large-scale pollution around 2000. It also indicated that agricultural production did not enter into mechanical automation and scale during this period, and there was no large-scale use of chemical fertilizers. In contrast, in 2014, the correlation between the environmental indicators in the groundwater of the Lalin River basin and the groundwater ions was high, especially the two ions,  $\text{Mg}^{2+}$  and  $\text{NO}_3^-$ , and the environmental factors of the environmental groundwater. This suggests that agricultural production had a greater impact on groundwater during this time period. The expansion of agricultural production and the increase in agricultural automation have increased the production of agricultural products and, at the same time, led to the entry of excessive nutrients from fertilizers into groundwater, which eventually caused the increase in groundwater pollution.

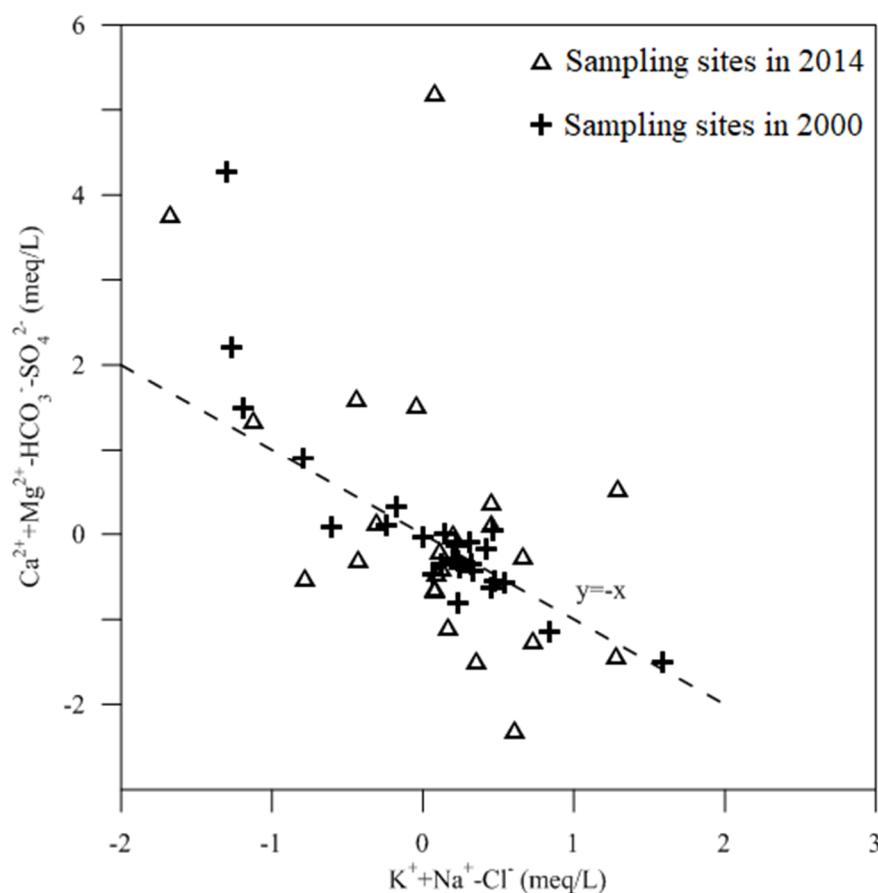


**Figure 6.** The plot of  $\text{HCO}_3^-$  and  $\text{SO}_4^{2-}$ -corrected  $\text{Ca}^{2+} + \text{Mg}^{2+}$  versus  $\text{Cl}^-$ -corrected  $\text{Na}^+$  of groundwater in the Lalin River Basin.

The correlation between  $\text{Mg}^{2+}$  and  $\text{NO}_3^-$ , which are the main substances in chemical fertilizers, and other environmental factors has increased, suggesting that crude agricultural management can cause increased groundwater pollution, requiring managers to pay attention to the impact of agricultural production on the groundwater environment while focusing on the growth of agricultural production (Figure S1). The modern agricultural production system indicates that the crude management is no longer suitable for the economic development, and the future refined agricultural production is the mainstream international research direction.

#### 4. Discussion

##### 4.1. Groundwater Pollution Assessment

The important parameters of TH, TDS,  $\text{Cl}^-$ ,  $\text{SO}_4^{2-}$ , and  $\text{NO}_3^-$  in 2000 and 2014 were selected to perform the comprehensive evaluation method. The assessment results clearly demonstrated that 70.4%, 18.5%, 3.7%, and 7.4% of the total shallow groundwater samples in 2000 were excellent, good, fair, and poor, respectively. Overall, 92.59% of the groundwater samples were considered to be suitable for drinking purposes, and the other groundwater samples were unfit for drinking purposes. In contrast, 34.8% of the total shallow groundwater samples in 2014 were excellent, 26.1% of groundwater samples were good, and 4.3% of the groundwater samples were fair and suitable for drinking. However, the groundwater samples that were unfavorable for drinking accounted for 34.8% of the total groundwater samples in 2014. Figure S2 showed that the poor water was mainly located near wells 4#, 10#, 11#, and 19#, where agricultural activities were intense.

Based on the above results, the groundwater quality of the study area gradually worsened, mainly influenced by the concentration of  $\text{NO}_3^-$ . Figure 1 showed that the

croplands were the dominant types of the land used in the study area, indicating that the concentrations of  $\text{NO}_3^-$  were derived from the agricultural activities, including the use of fertilizers, wastewater irrigation, and breakdown of crop remnants. In detail, the excessive use of nitrogen, such as ammonium nitrate and ammonium sulfate, within the conventional agriculture framework of the study area, played a significant role in the increase in the concentration of  $\text{NO}_3^-$ .

Statistical analysis of shallow groundwater samples showed that the relative concentrations of cations and anions in 2014 were in the following order:  $\text{Ca}^{2+} > \text{Na}^+ > \text{Mg}^{2+} > \text{K}^+$  and  $\text{HCO}_3^- > \text{SO}_4^{2-} > \text{Cl}^- > \text{NO}_3^-$  for cations and anions, respectively. The spatial distribution patterns of  $\text{K}^+$  and  $\text{NO}_3^-$  had no obvious regularity, whereas  $\text{Cl}^-$  and  $\text{Na}^+$  showed similar spatial distribution patterns. The concentrations of  $\text{Ca}^{2+}$ ,  $\text{Mg}^{2+}$ , and  $\text{HCO}_3^-$  increased from the Lalin River to the Mangniu River. A high concentration of  $\text{SO}_4^{2-}$  was distributed in areas close to the Lalin and Mangniu Rivers. Ca- $\text{HCO}_3$  and mixed-type water were the dominant hydro-chemical types. The analysis of the SI values for minerals and the Gibbs plot illustrated that the concentrations of major components were mainly controlled by rock weathering, such as the dissolution of calcite, dolomite, halite, gypsum, and aragonite, followed by ion exchange. Combined with the contaminant sources of the study area, indicators such as TH, TDS,  $\text{Cl}^-$ ,  $\text{SO}_4^{2-}$ , and  $\text{NO}_3^-$  were chosen to assess the quality of shallow groundwater using the comprehensive evaluation method. The results revealed that two groundwater samples in the study area were unfit for drinking, accounting for 7.4% of the total shallow groundwater samples, and the other samples were suitable for drinking use in 2000. In contrast, eight samples, approximately 34.8% of the total samples, were unsuitable for drinking in 2014.  $\text{NO}_3^-$  pollution from the excessive use of agricultural fertilizer was the dominant threat to groundwater quality in the study area. The study indicated that the concentrations of the major components in the riverside source of Wuchang were controlled by both natural and agricultural processes. Changes in anthropogenic activities should be taken into consideration to improve the groundwater quality.

By comparing several groundwater pollution evaluation methods, it was found that the overall differences between the methods were not significant, but the evaluation results differed at the more seriously polluted sampling sites. From Table 2, we could find that the evaluation results obtained by using the two improved mathematical methods were more accurate and reflected the actual situation of the evaluation area than before the improvement. For example, the groundwater contamination at points 4, 10, and 11 were the most serious among all sampling points. Regardless of the comprehensive evaluation method or the two improved mathematical evaluation methods, the groundwater contamination levels at these three study sample sites were below Level 3. The mutual verification between these three methods showed the scientific accuracy of the evaluation of the groundwater pollution status in the Lalin River basin. From the comparative analysis, it was also possible that the main groundwater pollution sources in the Lalin River basin were the above three sampling sites. These three sampling sites may be located at groundwater pooling areas or surface pollution accumulation areas.

Table 2 also illustrated that the improved groundwater pollution evaluation method has more detailed evaluation levels than the previous evaluation method and was more able to indicate the detailed situation of groundwater pollution in the area. From the previous single five-level evaluation criteria to the refined numerical criteria in this study, the evaluation criteria within the same level were refined on top of the levels available for classification, which provided effective data support for the future refinement and standardization of groundwater pollution management, and could also provide clearer directions for groundwater pollution management. From the methodological point of view, the improved method can further improve the management of groundwater pollution and provide a reference method for the calculation and analysis of the spatial distribution of groundwater on a large scale. For example, the groundwater pollution levels of site 16 and 17 were moderately polluted, calculated through the maximum affiliation, traditional gray

correlation, improved gray correlation, and traditional fuzzy mathematical method, and distinguished as invalid, while the improved fuzzy mathematical method distinguished the above two clearly and facilitates managers to adopt different control strategies.

**Table 2.** Comparison of groundwater water pollution evaluation results of different methods in the Lalin River Basin.

Site	Affiliation					A *	B *	C *	D *	E *
	I	II	III	IV	V					
1	0.394	0.333	0.218	0.058	0	0.394	IV	3	III	3.549
2	0.579	0.226	0.067	0.018	0.112	0.579	III	3	II	3.016
3	0.188	0.296	0.288	0.121	0.107	0.296	III	3	III	3.608
4	0	0.202	0.091	0.205	0.507	0.507	V	4	IV	3.902
5	0	0	0.333	0.455	0.212	0.455	III	3	III	2.678
6	0.012	0.496	0.123	0.369	0	0.496	III	3	III	3.142
7	0	0.268	0.396	0.082	0.254	0.396	II	3	III	3.401
8	0.089	0.471	0	0.219	0.621	0.221	II	3	III	2.223
9	0.109	0	0	0.672	0.219	0.219	I	2	III	2.759
10	0.315	0.175	0.302	0.088	0.195	0.315	III	3	IV	3.402
11	0.241	0.351	0.074	0	0.335	0.335	IV	3	III	3.215
12	0.743	0.063	0.136	0.058	0	0.743	I	2	II	2.000
13	0.481	0.352	0.149	0.018	0	0.481	III	3	III	3.423
14	0.125	0.379	0.343	0.153	0	0.379	II	3	II	1.643
15	0.187	0.212	0.601	0	0	0.601	I	2	I	1.025
16	0.315	0.585	0.089	0.011	0	0.585	III	3	III	2.907
17	0.305	0.212	0.387	0.096	0	0.387	III	3	III	2.659
18	0.254	0.128	0	0.116	0.546	0.546	I	2	I	1.074
19	0.521	0.081	0	0	0.398	0.521	II	3	II	1.686
20	0.709	0	0	0.185	0.106	0.709	III	3	III	3.566
21	0.423	0.312	0.058	0.207	0	0.423	II	3	II	2.341
22	0.305	0.212	0.387	0.096	0	0.387	III	3	III	2.659
23	0.179	0.629	0	0.177	0.015	0.629	IV	3	III	3.335

\* A is Maximum affiliation, B is Traditional gray correlation, C is Improving gray correlation, D is Traditional fuzzy mathematical method, E is Improved fuzzy mathematical method.

#### 4.2. Groundwater Quality Priority Control and Management

Along with economic and agricultural development, problems of groundwater quality have become increasingly outstanding and seriously influence the security of drinking water. As mentioned above, approximately 34.8% of the total shallow groundwater samples in 2014 were contaminated in the study area. Anthropogenic activities drastically affected the concentrations of major components in groundwater due to changes in the local hydrodynamic conditions. The wells of the residential drinking water might be easily polluted by the sewage discharge of croplands and domestic sewage. As a consequence, integrated water management for drinking and agricultural uses was an effective approach to solve the problems. A sustainable monitoring plan and technology for the removal of Fe and Mn must be taken into consideration. Moreover, biological fertilizers instead of chemical fertilizers should be used to decrease agricultural pollution.

Economic development has had a serious impact on groundwater resources that are rapidly being depleted in areas of major agricultural production [37–39]. The threat of groundwater contamination is particularly severe in areas with relatively shallow water tables and relatively high aquifer thickness. A combination of improved computational methods, including water chemistry investigations, as well as statistical and geostatistical techniques, was used in this study to analyze the impact of agricultural production on groundwater contamination in northeastern China. Groundwater chemistry studies have shown that agricultural activities and land use have a significant impact on nitrate concentrations in groundwater, and that nitrate accumulation in the groundwater environment can also occur due to tillage activities and unremediated [40,41] sewage systems, among

others. In addition, the comparative study of multiple methods proved the feasibility of using multiple precision evaluation methods for groundwater refinement management.

In northeastern China, open-weld rough agricultural operation management caused serious local groundwater pollution due to historical reasons. The multiple-calculation improvement model proposed in this study can effectively improve the groundwater pollution evaluation accuracy, which provides a scientific calculation basis for the input of groundwater management. The use of the new methods for groundwater analysis may allow government managers to distribute the funding more efficiently among the contaminated zones and thus reach better remediation results [42]. From a management perspective, this can also provide managers with ideas for large-scale groundwater management, saving society, government, and individual input.

## 5. Conclusions

We analyzed the chemical characteristics of shallow groundwater in the Lalin River basin, a typical black soil agricultural growing area in northeastern China, and evaluated the groundwater pollution status in the study area using an improved joint method. The area is a region of rapid agricultural development, and rapidly growing agricultural activities have led to water stress. The groundwater quality in the study area is generally above good, but below good in the groundwater quality of irrigation canals for agricultural cultivation. The chemical composition of groundwater in the Lalin River basin reflects a variety of sources and processes, including drinking into the gods, mineral dissolution, and fertilization. Groundwater contamination levels are highest in irrigated agricultural areas and are increasing further as the extent of agricultural production increases. The area of groundwater contamination in the region is also increasing with the observed trend of increasing land use and agricultural activities. The aquifer in the Lalin River basin is at risk of long-term contamination by human activities, so it is recommended to try strategic management to reduce irreversible contamination. In particular, the construction of an improved refined study methodology can provide a basis for a long-term effective strategy implementation for groundwater management in the Lalin River Basin.

**Supplementary Materials:** The following supporting information can be downloaded at: <https://www.mdpi.com/article/10.3390/su14116527/s1>.

**Author Contributions:** R.C.: Investigation, Data Curation, Writing—Original Draft Preparation. L.L.: Conceptualization, Methodology, Writing—Original Draft Preparation. Y.L.: Writing—Review and Editing. Y.Z.: Writing—Review and Editing. H.C.: Writing—Review and Editing. B.H.: Writing—Review and Editing. Q.Z.: Data Curation. Y.T.: Supervision, Project Administration. All authors have read and agreed to the published version of the manuscript.

**Funding:** This study was supported by National Natural Science Foundation of China (41877355), International Science and Technology Innovation Program of Chinese Academy of Agricultural Sciences (CAAS-ZDRW202110), and Beijing Advanced Innovation Program for Land Surface Science.

**Informed Consent Statement:** Informed consent was obtained from all subjects involved in the study.

**Data Availability Statement:** Not applicable.

**Acknowledgments:** The authors acknowledge the support by National Natural Science Foundation of China (41877355), International Science and Technology Innovation Program of Chinese Academy of Agricultural Sciences (CAAS-ZDRW202110), and Beijing Advanced Innovation Program for Land Surface Science.

**Conflicts of Interest:** The authors declare no conflict of interest.

## References

1. Liu, M.; Xiao, C.; Liang, X.; Wei, H. Response of groundwater chemical characteristics to land use types and health risk assessment of nitrate in semi-arid areas: A case study of Shuangliao City, Northeast China. *Ecotoxicol. Environ. Saf.* **2022**, *236*, 113473. [[CrossRef](#)]
2. Ma, J.; Ding, Z.; Wei, G.; Zhao, H.; Huang, T. Sources of water pollution and evolution of water quality in the Wuwei basin of Shiyang river, Northwest China. *J. Environ. Manag.* **2009**, *90*, 1168–1177. [[CrossRef](#)] [[PubMed](#)]
3. Ma, Y.; Liu, Z.H.; Xi, B.D.; He, X.S.; Li, Q.L.; Qi, Y.J.; Jin, M.Y.; Guo, Y. Characteristics of groundwater pollution in a vegetable cultivation area of typical facility agriculture in a developed city. *Ecol. Indic.* **2019**, *105*, 709–716. [[CrossRef](#)]
4. Zhao, B.; Sun, Z.; Liu, Y. An overview of in-situ remediation for nitrate in groundwater. *Sci. Total Environ.* **2022**, *804*, 149981. [[CrossRef](#)] [[PubMed](#)]
5. Zhao, X.; Wang, D.; Xu, H.; Ding, Z.; Shi, Y.; Lu, Z.; Cheng, Z. Groundwater pollution risk assessment based on groundwater vulnerability and pollution load on an isolated island. *Chemosphere* **2022**, *289*, 133134. [[CrossRef](#)] [[PubMed](#)]
6. Zhai, Y.; Lei, Y.; Zhou, J.; Li, M.; Wang, J.; Teng, Y. The spatial and seasonal variability of the groundwater chemistry and quality in the exploited aquifer in the Daxing District, Beijing, China. *Environ. Monit. Assess.* **2015**, *187*, 43. [[CrossRef](#)]
7. Zhang, B.; Song, X.; Zhang, Y.; Han, D.; Tang, C.; Yu, Y.; Ma, Y. Hydrochemical characteristics and water quality assessment of surface water and groundwater in Songnen plain, Northeast China. *Water Res.* **2012**, *46*, 2737–2748. [[CrossRef](#)]
8. Zhang, H.; Cheng, S.; Li, H.; Fu, K.; Xu, Y. Groundwater pollution source identification and apportionment using PMF and PCA-APCA-MLR receptor models in a typical mixed land-use area in Southwestern China. *Sci. Total Environ.* **2020**, *741*, 140383. [[CrossRef](#)]
9. Böhlke, J.-K. Groundwater recharge and agricultural contamination. *Hydrogeol. J.* **2002**, *10*, 153–179. [[CrossRef](#)]
10. Dhimmal, J.B.; Singh, S.S. Assessment of groundwater quality and its suitability for drinking and agriculture uses. *Int. J. Adv. Res.* **2014**, *2*, 77–87.
11. Adimalla, N.; Qian, H.; Nandan, M.J. Groundwater chemistry integrating the pollution index of groundwater and evaluation of potential human health risk: A case study from hard rock terrain of south India. *Ecotoxicol. Environ. Saf.* **2020**, *206*, 111217. [[CrossRef](#)] [[PubMed](#)]
12. El Alfy, M.; Lashin, A.; Abdalla, F.; Al-Bassam, A. Assessing the hydrogeochemical processes affecting groundwater pollution in arid areas using an integration of geochemical equilibrium and multivariate statistical techniques. *Environ. Pollut.* **2017**, *229*, 760–770. [[CrossRef](#)] [[PubMed](#)]
13. Gu, H.; Chi, B.; Li, H.; Jiang, J.; Qin, W.; Wang, H. Assessment of groundwater quality and identification of contaminant sources of Liujiang basin in Qinhuangdao, North China. *Environ. Earth Sci.* **2015**, *73*, 6477–6493. [[CrossRef](#)]
14. Alaa, A.; Masoud, A.A. Groundwater quality assessment of the shallow aquifers west of the Nile Delta (Egypt) using multivariate statistical and geostatistical techniques. *J. Afr. Earth Sci.* **2014**, *95*, 123–137.
15. Arumugam, K.; Elangovan, K. Hydrochemical characteristics and groundwater quality assessment in Tirupur Region, Coimbatore District, Tamil Nadu, India. *Environ. Earth Sci.* **2009**, *58*, 1509. [[CrossRef](#)]
16. Augustsson, A.; Söderberg, T.U.; Fröberg, M.; Kleja, D.B.; Åström, M.; Svensson, P.A.; Jarsjö, J. Failure of generic risk assessment model framework to predict groundwater pollution risk at hundreds of metal contaminated sites: Implications for research needs. *Environ. Res.* **2020**, *185*, 109252. [[CrossRef](#)] [[PubMed](#)]
17. Haghazadeh, H.; Johannesson, K.H.; González-Pinzón, R.; Pourakbar, M.; Aghayani, E.; Rajabi, A.; Hashemi, A.A. Groundwater geochemistry, quality, and pollution of the largest lake basin in the Middle East: Comparison of PMF and PCA-MLR receptor models and application of the source-oriented HHRA approach. *Chemosphere* **2022**, *288*, 132489. [[CrossRef](#)]
18. Moussa, A.B.; Mzali, H.; Zouari, K.; Hezzi, H. Hydrochemical and isotopic assessment of groundwater quality in the Quaternary shallow aquifer, Tazoghrane region, north-eastern Tunisia. *Quat. Int.* **2014**, *338*, 51–58. [[CrossRef](#)]
19. Nagaraju, A.; Sreedhar, Y.; Kumar, K.S.; Thejasw, A.; Sharifi, Z. Assessment of groundwater quality and evolution of hydrochemical facies around Tummalapalle Area, Cuddapah District, Andhra Pradesh, South India. *Environ. Anal. Chem.* **2014**, *1*, 1–6.
20. Liu, L.; Zhou, J.; An, X.; Zhang, Y.; Yang, L. Using fuzzy theory and information entropy for water quality assessment in Three Gorges region, China. *Expert Syst. Appl.* **2010**, *37*, 2517–2521. [[CrossRef](#)]
21. Nazzal, Y.; Ahmed, I.; Al-Arifi, N.; Ghrefat, H.; Zaidi, F.K.; El-Waheidi, M.M.; Batayneh, A.; Zumlot, T. A pragmatic approach to study the groundwater quality suitability for domestic and agricultural usage, Saq aquifer, northwest of Saudi Arabia. *Environ. Monit. Assess.* **2014**, *186*, 4655–4667. [[CrossRef](#)] [[PubMed](#)]
22. Pathak, D.R.; Bhandary, N.P. Evaluation of groundwater vulnerability to nitrate in shallow aquifer using multi-layer fuzzy inference system within GIS environment. *Groundw. Sustain. Dev.* **2020**, *11*, 100470. [[CrossRef](#)]
23. Purushotham, D.; Prakash, M.R.; Rao, A.N. Groundwater depletion and quality deterioration due to environmental impacts in Maheshwaram watershed of R.R. district, AP (India). *Environ. Earth Sci.* **2011**, *62*, 1707–1721. [[CrossRef](#)]
24. Jasmin, I.; Mallikarjuna, P. Physicochemical quality evaluation of groundwater and development of drinking water quality index for Araniar River Basin, Tamil Nadu, India. *Environ. Monit. Assess.* **2014**, *186*, 935–948. [[CrossRef](#)]
25. Li, L.; Zou, S. Comparison of comprehensive index method and fuzzy comprehensive method in the evaluation of groundwater quality: A case study in Zunyi City. *Carsologica Sin.* **2014**, *33*, 22–30.

26. Rodriguez-Galiano, V.F.; Luque-Espinar, J.A.; Chica-Olmo, M.; Mendes, M.P. Feature selection approaches for predictive modelling of groundwater nitrate pollution: An evaluation of filters, embedded and wrapper methods. *Sci. Total Environ.* **2018**, *624*, 661–672. [[CrossRef](#)]
27. Schot Paul, P.; Pieber Simone, M. Spatial and temporal variations in shallow wetland groundwater quality. *J. Hydrol.* **2012**, *422–423*, 43–52. [[CrossRef](#)]
28. Sege, J.; Ghanem, M.; Ahmad, W.; Bader, H.; Rubin, Y. Distributed data collection and web-based integration for more efficient and informative groundwater pollution risk assessment. *Environ. Model. Softw.* **2018**, *100*, 278–290. [[CrossRef](#)]
29. Huan, H.; Hu, L.; Yang, Y.; Jia, Y.; Lian, X.; Ma, X.; Xi, B. Groundwater nitrate pollution risk assessment of the groundwater source field based on the integrated numerical simulations in the unsaturated zone and saturated aquifer. *Environ. Int.* **2020**, *137*, 105532. [[CrossRef](#)]
30. Jankowski, J.; Acworth, R.I.; Shekarforoush, S. Reverse ion exchange in deeply weathered porphyritic dacite fractured aquifer system, Yass, New South Wales, Australia. In *Water-Rock Interaction, Proceedings of the 9th International Symposium on Water-Rock Interaction, Taupo, New Zealand, 30 March–3 April 1998*; Arehart, G.B., Hulston, J.R., Eds.; AA Balkema: Rotterdam, The Netherlands, 1998; pp. 243–246.
31. Rajendra Prasad, D.S.; Sadashivaiah, C.; Rangna, G. Hydrochemical characteristics and evaluation of groundwater quality of Tumkur Amanikere lake Watershed, Karnataka. *India. E-J. Chem.* **2009**, *6* (Suppl. S1), S211–S218. [[CrossRef](#)]
32. Ramesh, S.; Sukumaran, N.; Murugesan, A.; Rajan, M. An innovative approach of Drinking Water Quality Index—A case study from Southern Tamil Nadu, India. *Ecol. Indic.* **2010**, *10*, 857–868. [[CrossRef](#)]
33. Ranjan, R.K.; Ramanathan, A.L.; Parthasarathy, P.; Kumar, A. Hydrochemical characteristics of groundwater in the plains of Phalgu River in Gaya, Bihar, India. *Arab. J. Geosci.* **2013**, *6*, 3257–3267. [[CrossRef](#)]
34. Sharif, M.; Davis, R.; Steele, K.; Kim, B.; Kresse, T.; Fazio, J. Inverse geochemical modeling of groundwater evolution with emphasis on arsenic in the Mississippi River Valley alluvial aquifer, Arkansas (USA). *J. Hydrol.* **2008**, *350*, 41–55. [[CrossRef](#)]
35. Singh, P.; Tiwari, A.; Singh, P.K. Assessment of groundwater quality of Ranchi township area, Jharkhand, India by using Water Quality Index method. *Int. J. Chem. Tech. Res.* **2015**, *7*, 73–79.
36. Zhang, Q.; Li, P.; Lyu, Q.; Ren, X.; He, S. Groundwater contamination risk assessment using a modified DRATICL model and pollution loading: A case study in the Guanzhong Basin of China. *Chemosphere* **2022**, *291*, 132695. [[CrossRef](#)]
37. Ren, G.; Zhao, C.; Sun, X. Analysis and evaluation of groundwater quality of Qijia reserve water source of Changchun city, Jilin province. *Jilin Geol.* **2014**, *33*, 98–102.
38. Sitambuk-Giljanovic, N. Water quality evaluation by index in Dalmatia. *Water Res.* **1999**, *33*, 3423–3440. [[CrossRef](#)]
39. Subba Rao, N.; Dinakar, A.; Sun, L. Estimation of groundwater pollution levels and specific ionic sources in the groundwater, using a comprehensive approach of geochemical ratios, pollution index of groundwater, unmix model and land use/land cover—A case study. *J. Contam. Hydrol.* **2022**, *248*, 103990. [[CrossRef](#)]
40. Wu, W.; Liao, R.; Hu, Y.; Wang, H.; Liu, H.; Yin, S. Quantitative assessment of groundwater pollution risk in reclaimed water irrigation areas of northern China. *Environ. Pollut.* **2020**, *261*, 114173. [[CrossRef](#)]
41. Yu, L.; Zheng, T.; Zheng, X.; Hao, Y.; Yuan, R. Nitrate source apportionment in groundwater using Bayesian isotope mixing model based on nitrogen isotope fractionation. *Sci. Total Environ.* **2020**, *718*, 137242. [[CrossRef](#)]
42. Zghibi, A.; Merzougui, A.; Zouhri, L.; Tarhouni, J. Understanding groundwater chemistry using multivariate statistics techniques to the study of contamination in the Korba unconfined aquifer system of Cap-Bon (North-east of Tunisia). *J. Afr. Earth Sci.* **2014**, *89*, 1–15. [[CrossRef](#)]